Collapse of Axially Compressed Cylindrical Shells with Random Imperfections

J. Arbocz* and J. M. A. M. Hol†
Delft University of Technology, Delft, The Netherlands

The establishment of an International Imperfection Data Bank is discussed. Characteristic initial imperfection distributions associated with different fabrication techniques are shown. Using the first-order, second-moment analysis, a stochastic method is presented, whereby the stability of isotropic, orthotropic, and anisotropic nominally circular cylindrical shells under axial compression, external pressure, and/or torsion possessing general nonsymmetric random initial imperfections can be evaluated. Results of measurements of initial imperfections are represented in Fourier series and the Fourier coefficients are used to construct the second-order statistical properties needed. The computation of the buckling loads is done with standard computer codes and includes a rigorous satisfaction of the specified boundary conditions. It is shown that the proposed stochastic approach provides a means to combine the latest theoretical findings with the practical experiences spanning about 75 years in an optimal manner via the advanced computational facilities currently available.

I. Introduction

WITH the arrival of the era of supercomputing there is a tendency to replace the relatively expensive experimental investigations by numerical simulation. The use of large general purpose computer codes for the analysis of different types of aerospace, marine, and civil engineering structures is by now well accepted. These programs have been used successfully to calculate the stress and deformation patterns of very complicated structural configurations with the accuracy demanded in engineering analysis.

However, there exist numerous complex physical phenomena where only a combined experimental, analytical, and numerical procedure can lead to an acceptable solution. One such problem is the prediction of the behavior of buckling sensitive structures under the different loading conditions that can occur in everyday usage.

The axially compressed cylindrical shell represents one of the best known examples of the very complicated stability behavior that can occur with thin-walled structures. For thin shells that buckle elastically initial geometric imperfections[1,2] and the effect of the different boundary conditions[3-5] have been identified as the main cause for the wide scatter of the experimental results. However, this knowledge has not been, as yet, incorporated into the current shell design manuals.

These design recommendations[6-8] all adhere to the so-called lower bound design philosophy and as such recommend the use of the following buckling formula:

$$P_a \leq \frac{\gamma}{F.S.} P_{\text{crit}} \tag{1}$$

where P_a = allowable applied load; P_{crit} = lowest buckling load of the perfect structure; γ = "knockdown factor"; and $F.S.$ = factor of safety.

The empirical knockdown factor γ is so chosen that when it is multiplied with P_{crit}, the lowest buckling load of the perfect structure, a lower bound to all available experimental data is obtained. For isotropic shells under axial compression this approach yields the lower bound curve[9] shown in Fig. 1.

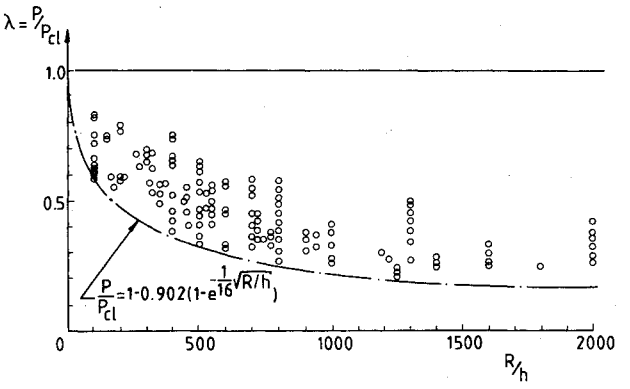

Fig. 1 Test data for isotropic cylinders under axial compression.[9]

It has been hoped that with the large-scale introduction of advanced computer codes, which incorporate the latest theoretical findings, an alternate design approach could be developed that would no longer penalize innovative shell design because of the poor experimental results obtained elsewhere. The main difficulty in applying these new analysis procedures lies in the fact that they require some advanced knowledge of the initial geometric imperfections of the structure under consideration, which is rarely available. For a prototype the imperfections can be measured experimentally and then they can be incorporated into the theoretical analysis to predict the buckling load accurately. This approach, however, is impractical for the prediction of the buckling load of shells manufactured in normal production runs. The best one can hope to do for these shells is to establish the characteristic initial imperfection distribution[10-12] that a given fabrication process is likely to produce, and then to combine this information with some kind of statistical analysis of both the initial imperfections and the corresponding critical loads, a kind of statistical imperfection-sensitivity analysis.

The central goal of the shell research reported in this paper is the development of "improved shell design criteria." The improvements with respect to the presently recommended shell design procedures are primarily sought in a more selective approach by the definition of the "knockdown" factor γ. Thus, for instance, if a company takes great care in producing its shells very accurately, and if it can show experimentally that the boundary conditions are defined in such a way that

Received Jan. 7, 1991; revision received April 5, 1991; accepted for publication April 5, 1991.

*Professor of Aircraft Structures, Faculty of Aerospace Engineering.

†Assistant Professor, Faculty of Aerospace Engineering.

no additional imperfections (especially at the shell edges) are introduced, then the use of an "improved (higher) knockdown" factor λ_a derived by a stochastic approach should be allowed. The proposed new improved shell design procedure can be represented by the following formula:

$$P_a \leq \frac{\lambda_a}{F.S.} P_c \tag{2}$$

where P_a = allowable applied load; P_c = lowest buckling load of the "perfect" structure computed via one of the shell codes; λ_a = reliability-based improved (higher) knockdown factor; and $F.S.$ = factor of safety.

The steps involved in the derivation of such a reliability-based improved (higher) knockdown factor λ_a are the subject of this paper.

II. Characteristic Imperfection Distributions

The use of the proposed statistical imperfection-sensitivity analysis depends strongly on the availability of the so-called characteristic initial imperfection distributions. Thus the critical question is: Can one associate characteristic initial imperfection distributions with a specified manufacturing process? That the answer to this question is an unconditional yes will be demonstrated by a few examples.

A. Laboratory Scale Shells

Figure 2 shows the measured initial imperfections of the integrally stringer stiffened aluminum shell AS-2, which has been tested at Caltech.[13] Figure 3 shows the measured initial imperfections of a similar shell KR-1 tested at Technion.[11] For further analysis the measured initial imperfections are decomposed in a half-wave sine Fourier series

$$\overline{W}(x,y) = h \sum_{k=1}^{n1} \sum_{l=1}^{n2} \sin\frac{k\pi x}{L}\left(C_{kl}\cos\frac{ly}{R} + D_{kl}\sin\frac{ly}{R}\right) \tag{3}$$

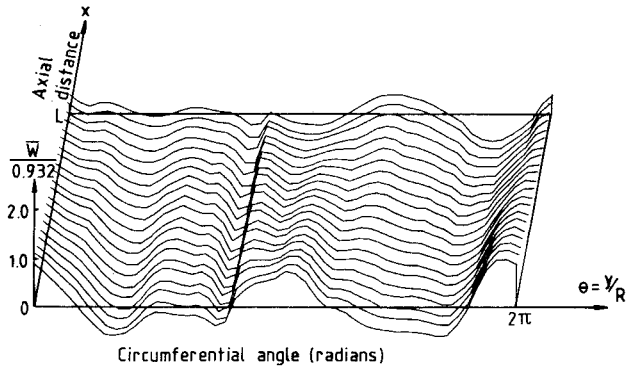

Fig. 2 Measured initial shape of the stringer stiffened shell AS-2.[13]

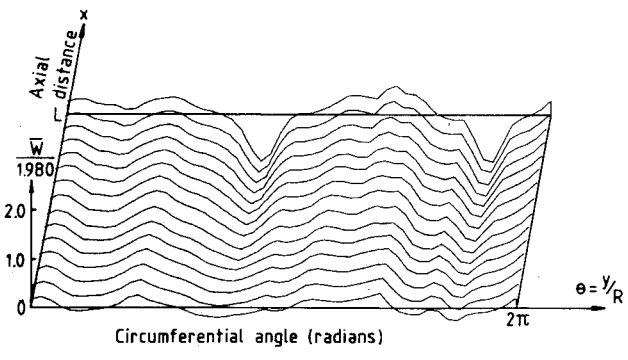

Fig. 3 Measured initial shape of the stringer stiffened shell KR-1.[11]

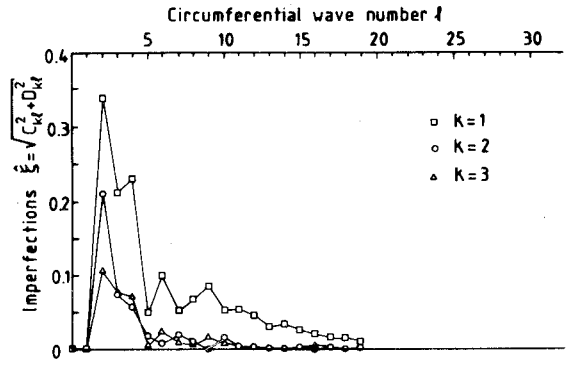

Fig. 4 Circumferential variation of the half-wave sine Fourier representation (Shell AS-2).

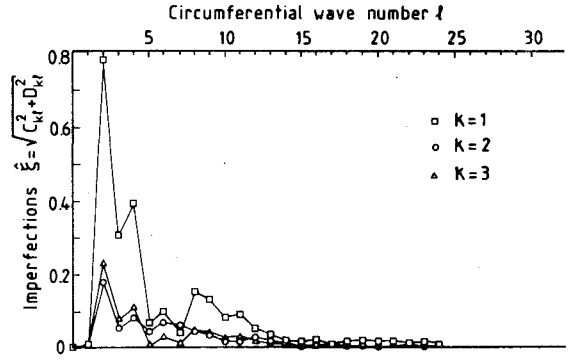

Fig. 5 Circumferential variation of the half-wave sine Fourier representation (Shell KR-1).

where h is the skin thickness and not some "effective" thickness including the stringers.

For the sake of comparison Figs. 4 and 5 display the variation of the measured half-wave sine Fourier coefficients as a function of the circumferential wave numbers l for selected axial half-wave numbers k, for the shells AS-2 and KR-1. As one can see in both cases the amplitudes of the Fourier coefficients decay with increasing wave numbers both in the axial and in the circumferential directions. The Donnell-Imbert[14] analytical imperfection model

$$\bar{\xi}_{kl} = \sqrt{C_{kl}^2 + D_{kl}^2} = \frac{\overline{X}}{k^r l^s} \tag{4}$$

where the coefficients $\overline{X}$, r, and s are determined by least squares fitting the measured imperfection data displayed in Figs. 4 and 5, represents the variation of the harmonic components with axial (k) and circumferential (l) wave numbers satisfactorily. Since both shells were machined out of seamless thick-walled 6061-T6 aluminum alloy tubing, therefore the imperfection model given by Eq. (4) represents the characteristic imperfection distribution for this fabrication process.

B. Full-Scale Shells

Turning now to large-scale or full-scale shells, Fig. 6 shows the three-dimensional plot of the measured initial imperfections of a large-scale shell (945.8 mm radius, 0.635 mm wall thickness, 2743.2 mm length) tested at the Georgia Institute of Technology.[15] This shell was assembled from six identical longitudinal panels and reinforced by 312 closely spaced Z-shape stringers on the inside. The edges of the panels were jointed by offset lap splices with stringers riveted along each joint line. The shell was held circular by means of heavy rolled

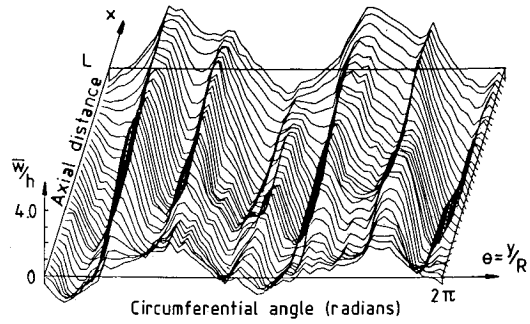

Fig. 6 Measured initial shape of Horton's shell HO-1.[15]

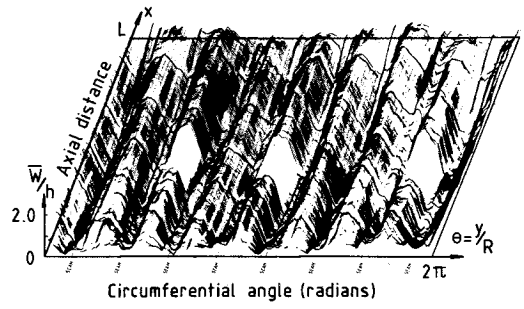

Fig. 8 Measured initial shape of the ARIANE Shell AR23-1.[16]

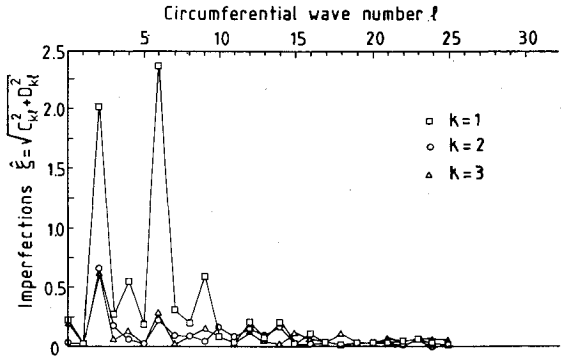

Fig. 7 Circumferential variation of the half-wave sine Fourier representation (Shell HO-1).

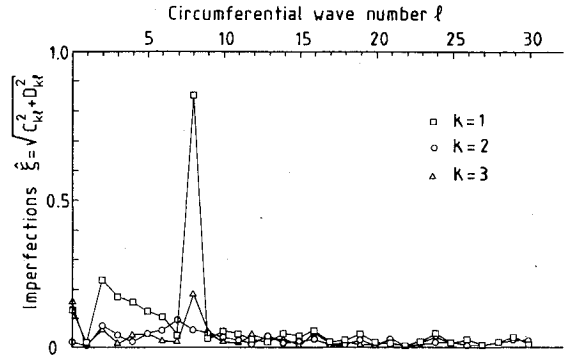

Fig. 9 Circumferential variation of the half-wave sine Fourier representation (Shell AR23-1).

bracket-shape external frames located 3.175 mm from each shell end. In addition seven Z-shape equally spaced rings were riveted to the outer skin. It can clearly be seen from Fig. 7 that the amplitudes of the Fourier harmonics with a single half-wave in the axial direction have two distinct maxima, one at $l = 2$ (out of roundness) and another at $l = 6$ (number of panels the shell is assembled from). The Fourier coefficients with more than a single half-wave in the axial direction are in comparison much smaller.

In the last few years a number of imperfection surveys on the Ariane interstage I/II and II/III shells have been carried out.[16] Figure 8 shows the three-dimensional plot of the Ariane interstage II/III shell AR23-1 (1300.0 mm radius, 1.2 mm wall thickness, 2730.0 mm length). These shells are assembled out of eight identical longitudinal panels. Adjacent panels are jointed by offset lap splices and one of the 120 equally spaced hat-shape stringers is riveted along the joint line on the outside. The shells are held circular by two precision-machined end-rings on the outside and five equally spaced bracket-shape rings on the inside. As can be seen from Fig. 9 the amplitudes of the Fourier harmonics with a single half-wave in the axial direction this time have a distinct maximum at $l = 8$ (which corresponds to the number of panels the shell is assembled from). There is also a sizable $l = 2$ (out of roundness) component. All other Fourier coefficients are in comparison much smaller.

Thus, as has been pointed out by the first author in a survey lecture,[10] it appears from the results presented in Figs. 7 and 9 that for full-scale aerospace shells assembled out of a fixed number of curved panels the initial imperfections will be dominated by two components only, if the joints are riveted. Using the half-wave sine axial representation both components will have a single half-wave in the axial direction and, respectively, two and N_p full-waves in the circumferential direction, where N_p is the number of full-length panels out of which the shell is assembled. By using accurately machined rigid end rings the $l = 2$ (out of roundness) component can be significantly reduced in size. The variation of the measured Fourier coefficients with axial half-wave (k) and circumferential full-wave (l) numbers can be approximated by expressions of the following type:

$$\bar{\xi}_{kl} = \sqrt{C_{kl}^2 + D_{kl}^2} = \frac{1}{k^r}\left\{\frac{\bar{X}_1}{(l_1 - l)^2 + 2\zeta_1 l^2} + \frac{\bar{X}_2}{(l_2 - l)^2 + 2\zeta_2 l^2}\right\} \tag{5}$$

where the coefficients $\bar{X}_1, \bar{X}_2, r, l_1, l_2, \zeta_1$, and ζ_2 are determined by least squares fitting the measured data displayed in Figs. 7 and 9. Thus Eq. (5) represents the characteristic imperfection distribution of full-scale aerospace shells assembled out of a fixed number of full-length panels by riveted joints.

The above examples demonstrate unequivocally that indeed characteristic initial imperfection distributions can be associated with the different fabrication processes. It must also be clear that further advances toward more accurate buckling load predictions of thin shells depend on the availability of extensive information about realistic imperfections and their correlation with manufacturing processes. Hence the need for the establishment of an International Imperfection Data Bank.

The purpose of creating this International Imperfection Data Bank is twofold:

1) All the imperfection data obtained at different laboratories by different investigators are presented in identical format. This makes the comparison and the critical evaluation possible, resulting in characteristic imperfection distributions for the different manufacturing processes used.

2) For those who want to use the powerful nonlinear shell analysis codes on today's supercomputers, the much-needed realistic imperfection distributions are made available.

Besides contributions by Caltech, the TU-Delft, and Technion, the International Imperfection Data Bank contains results of initial imperfection surveys carried out at the University of Glasgow,[17] Det norske Veritas,[18] and others.

III. Stochastic Stability Analysis

A. Some General Concepts

It has been demonstrated in the previous section that, indeed, one can associate characteristic initial imperfection distributions with the different fabrication processes (see also Refs. 10–12). The question then arises: Given a characteristic initial imperfection distribution, how does one proceed to incorporate this knowledge into a systematic design procedure?

Since initial imperfections are obviously random in nature some kind of stochastic stability analysis is called for. The buckling of imperfection sensitive structures with small random initial imperfections has been studied by several investigators like Bolotin,[19] Fraser and Budiansky,[20] Amazigo,[21] Roorda,[22] and Hansen,[23] to name just a few. In the absence of experimental evidence about the type of imperfections that occur in practice and in order to reduce the mathematical complexity of the problem, all the above named investigators have worked with some form of idealized imperfection distribution.

In 1979 Elishakoff[24] proposed a generalization of the above methods which makes it possible to introduce the results of experimentally measured initial imperfections routinely into the analysis. The proposed approach is based on the notion of a reliability function $R(\lambda)$, where by definition

$$R(\lambda) = Prob(\Lambda \geq \lambda) \tag{6}$$

and λ = normalized load parameter ($= P/P_{cl}$) and Λ = normalized random buckling load.

As can be seen from Fig. 10 the knowledge of the reliability function permits the evaluation of the allowable load, defined as the load level λ_a for which the desired reliability is achieved, for a whole ensemble of similar shells produced by a given manufacturing process. Notice that the allowable load level λ_a is identical to the improved (higher) knockdown factor introduced in Eq. (2).

Initially Elishakoff suggested utilizing the Monte Carlo method to obtain the reliability function $R(\lambda)$ for a certain shell structure produced by a given fabrication process. In later papers it was shown that by replacing the Monte Carlo method by the first-order, second-moment method[25] the number of deterministic buckling load calculations needed to derive the reliability function $R(\lambda)$ is greatly reduced (from, say, 1089 to 13).

In the present paper it will be shown that by using the first-order, second-moment method[25,26] it is possible to develop a simple but rational method for checking the reliability of orthotropic shells using some statistical measures of the imperfections involved, and to provide an estimate of the structural reliability whereby also the specified boundary conditions are rigorously enforced.

B. First-Order, Second-Moment Method

The first-order, second-moment method is based on the state equation

$$Z = Z(X_1, X_2, \ldots, X_n) \tag{7}$$

where the nature of the so-called performance function $Z(\ldots)$ depends on the type of structure and the limit state considered, and where the basic random variables X_i are the Fourier coefficients of the initial imperfections. According to the definition of Z, the equation

$$Z = 0 \tag{8}$$

determines the failure boundary. Thus $Z < 0$ implies failure and $Z > 0$ indicates success. The use of the first-order, second-moment method then requires linearization of the function Z at the mean point and knowledge of the distribution of the random vector X. Calculations are relatively simple if X is normally distributed. If X is not normally distributed, an appropriate normal distribution has to be substituted instead of the actual one.

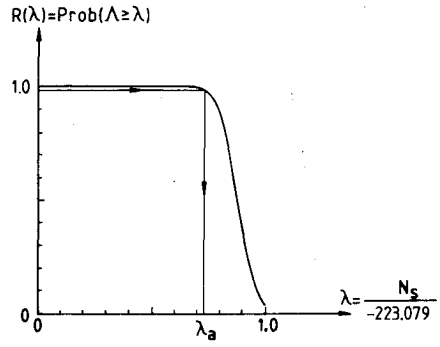

Fig. 10 Reliability curve calculated via the first-order, second-moment method (SS-3 boundary condition: $N_x = v = W = M_x = 0$).

In the present case one is interested in knowing the reliability $R(\lambda)$ of the structure at any given load λ; that is, one wants to obtain

$$R(\lambda) = Pr(\Lambda_s \geq \lambda) = \text{probability that } \Lambda_s \geq \lambda \tag{9}$$

In this case a function Z can be defined as

$$Z(\lambda) = \Lambda_s - \lambda = \Psi(X_1, X_2, \ldots, X_n) - \lambda \tag{10}$$

where Λ_s is the random buckling load and λ is the applied nondimensional deterministic load. It is apparent that in the absence of a straightforward deterministic relation connecting Λ_s and the X_i an analytical solution is unfeasible. However, the first-order, second-moment analysis can be done numerically, as has been reported in Ref. 26 for a different problem.

To combine the use of numerical codes with the mean value first-order, second-moment method one needs to know the lower order probabilistic characteristics of Z. In the first approximation the mean value of Z is determined as follows:

$$\begin{aligned} E(Z) &= E(\Lambda_s) - \lambda \\ &= E[\Psi(X_1, X_2, \ldots, X_n)] - \lambda \\ &\sim \Psi[E(X_1), E(X_2), \ldots, E(X_n)] - \lambda \end{aligned} \tag{11}$$

This corresponds to the use of the Laplace approximation of the moments of nonlinear functions. The value of

$$\Psi[E(X_1), E(X_2), \ldots, E(X_n)] \tag{12}$$

is calculated numerically by STAGS,[27] the code that was chosen for the numerical work. It corresponds to the deterministic buckling load of the structure possessing mean imperfection amplitudes.

The variance of Z is given by

$$\mathrm{Var}(Z) = \mathrm{Var}(\Lambda_s) \sim \sum_{j=1}^{n} \sum_{k=1}^{n} \left(\frac{\partial \Psi}{\partial \xi_j}\right)\left(\frac{\partial \Psi}{\partial \xi_k}\right) \mathrm{cov}(X_j, X_k) \tag{13}$$

where $\mathrm{cov}(X_j, X_k)$ is the variance-covariance matrix. The calculation of the derivatives $\partial\Psi/\partial\xi_j$ (or $\partial\Psi/\partial\xi_k$) is performed numerically by using the following numerical differentiation formula at values of $\xi_j = E(X_j)$ [or $\xi_k = E(X_k)$]:

$$\frac{\partial \Psi}{\partial \xi_j} = \frac{\Psi(\xi_1, \xi_2, \ldots, \xi_{j-1}, \xi_j + \Delta\xi_j, \xi_{j+1}, \ldots, \xi_n) - \Psi(\xi_1, \xi_2, \ldots, \xi_n)}{\Delta\xi_j} \tag{14}$$

Having obtained the quantities $E(Z) = E(\Lambda_s) - \lambda$ and $\mathrm{Var}(Z)$ one can estimate the probability of failure $P_F(\lambda)$ as

$$P_F(\lambda) = Pr(Z < 0) = F_Z(0) = \int_{-\infty}^{0} f_Z(t)\, dt \qquad (15)$$

where $F_Z(t)$ is the probability distribution function of Z and $f_Z(t)$ is the probability density function of Z.

Assuming that the performance function Z is normally distributed, then

$$f_Z(t) = \frac{1}{\sigma_Z\sqrt{2\pi}} \exp\left[-\frac{1}{2}\left(\frac{t-a}{\sigma_Z}\right)^2\right] \qquad (16)$$

where $a = E(Z)$ and $\sigma_Z = \sqrt{\mathrm{Var}(Z)}$. Further

$$F_Z(0) = \int_{-\infty}^{0} f_Z(t)\, dt = \frac{1}{2} + \mathrm{erf}\left(-\frac{a}{\sigma_Z}\right)$$

$$= \frac{1}{2} - \mathrm{erf}\left(\frac{a}{\sigma_Z}\right) = \phi(-\beta) \qquad (17)$$

where $\beta = a/\sigma_Z$ is the reliability index, $\phi(\beta)$ is the standard normal probability distribution function, and the error function $\mathrm{erf}(\beta)$ is defined as

$$\mathrm{erf}(\beta) = \frac{1}{\sqrt{2\pi}} \int_0^{\beta} e^{-t^2/2}\, dt \qquad (18)$$

Finally the reliability $R(\lambda)$ will be estimated as

$$R(\lambda) = 1 - P_F(\lambda) = 1 - Pr(Z < 0)$$

$$= 1 - F_Z(0) = \tfrac{1}{2} + \mathrm{erf}(\beta) = \phi(\beta) \qquad (19)$$

C. Statistical Measures of the Initial Imperfections

As can be seen from Eqs. 11 and 13, in order to be able to evaluate the mean value and the variance of the performance function Z, one must know the mean values and the variance-covariance matrix of the basic random variables X_i. Since in this case the basic random variables X_i represent the Fourier coefficients of the initial imperfections, the above statistical measures can only be evaluated if a sufficiently detailed initial imperfection data bank (see Refs. 28 and 29) is available.

Thus, if complete initial imperfection surveys have been carried out on a small sample of N nominally identical shells, then the measured data can be represented by the following truncated half-wave double Fourier series

$$\bar{w}^{(m)}(x, y) = h \sum_{i=1}^{n1} A_i^{(m)} \cos\frac{i\pi x}{L}$$

$$+ h \sum_{k=1}^{n} \sum_{l=1}^{n} \sin\frac{k\pi x}{L}\left(C_{kl}^{(m)} \cos\frac{ly}{R} + D_{kl}^{(m)} \sin\frac{ly}{R}\right) \qquad (20)$$

where $m = 1, 2, \ldots, N$. As pointed out in Refs. 28 and 29, the individual Fourier coefficients $A_i^{(m)}$, $C_{kl}^{(m)}$, and $D_{kl}^{(m)}$ can be evaluated numerically from the measured imperfections data by harmonic analysis. For the sake of simplicity one can write Eq. (20) in an alternate way, replacing the double summation in Eq. (20) by a single summation

$$\bar{w}^{(m)}(x, y) = h \sum_{i=1}^{n1} A_i^{(m)} \cos\frac{i\pi x}{L}$$

$$+ h \sum_{r=1}^{n2} \sin\frac{k_r\pi x}{L}\left(C_r^{(m)} \cos\frac{l_r y}{R} + D_r^{(m)} \sin\frac{l_r y}{R}\right) \qquad (21)$$

where $m = 1, 2, \ldots, N$. The quantities indexed by r are chosen so as to ensure the equivalence of the two series given by Eqs. (20) and (21) and $n_2 = n \cdot n$. Then for each shell the basic random variables are assigned as follows:

$$\begin{aligned} X_1 &= A_1 \quad X_2 = A_2 \quad \cdots \quad X_{n1} = A_{n1} \\ X_{n1+1} &= C_1 \quad \cdots \quad X_{n1+n2} = C_{n2} \\ X_{n1+n2+1} &= D_1 \quad \cdots \quad X_{n1+2n2} = D_{n2} \end{aligned} \qquad (22)$$

Their mean values are estimated by ensemble averaging yielding

$$E(X_i) = \frac{1}{N}\sum_{m=1}^{N} A_i^{(m)} \qquad i = 1, 2, \ldots, n_1$$

$$E(X_i) = \frac{1}{N}\sum_{m=1}^{N} C_i^{(m)} \qquad i = n_1 + 1, \ldots, n_1 + n_2$$

$$E(X_i) = \frac{1}{N}\sum_{m=1}^{N} D_i^{(m)} \qquad i = n_1 + n_2 + 1, \ldots, n_1 + 2n_2 \qquad (23)$$

In this case the variance-covariance matrix has the following structure

$$\mathrm{cov}(X_i, X_j) = \begin{Bmatrix} K_{ApAq} & K_{ApCs} & K_{ApDs} \\ K_{CrAq} & K_{CrCs} & K_{CrDs} \\ K_{DrAq} & K_{DrCs} & K_{DrDs} \end{Bmatrix} \qquad (24)$$

The elements of this matrix are once again estimated by using ensemble averaging. Thus

$$K_{ApAq} = \frac{1}{N-1}\sum_{m=1}^{N} [A_p^{(m)} - E(A_p)][A_q^{(m)} - E(A_q)] \qquad (25a)$$

$$K_{ApCs} = \frac{1}{N-1}\sum_{m=1}^{N} [A_p^{(m)} - E(A_p)][C_s^{(m)} - E(C_s)] \qquad (25b)$$

$$K_{ApDs} = \frac{1}{N-1}\sum_{m=1}^{N} [A_p^{(m)} - E(A_p)][D_s^{(m)} - E(D_s)] \qquad (25c)$$

$$K_{CrCs} = \frac{1}{N-1}\sum_{m=1}^{N} [C_r^{(m)} - E(C_r)][C_s^{(m)} - E(C_s)] \qquad (25d)$$

$$K_{CrDs} = \frac{1}{N-1}\sum_{m=1}^{N} [C_r^{(m)} - E(C_r)][D_s^{(m)} - E(D_s)] \qquad (25e)$$

$$K_{DrDs} = \frac{1}{N-1}\sum_{m=1}^{N} [D_r^{(m)} - E(D_r)][D_s^{(m)} - E(D_s)] \qquad (25f)$$

Notice that these quantities represent unbiased estimates. An advantage of this method is that the statistical parameters of the initial imperfections are estimated from the real measurements on the shell profiles. The only assumption made is that the Fourier coefficients have a multivariate normal distribution.

D. Calculation of Derivatives $\partial\Psi/\partial\xi_j$

As mentioned earlier the calculation of the derivatives $\partial\Psi/\partial\xi_j$ is done numerically by using the numerical differentiation formula given by Eq. (14). Thus, to find these derivatives, it is necessary to carry out collapse load calculations with mean imperfections. In this study the computation of the collapse loads is done with a modified finite difference version of the well-known code STAGS, which was originally developed in the early 1970s for the nonlinear collapse analysis of shells with general shapes.

The finite difference version of STAGS is based on a theory in which the shell surface is subdivided, by means of a finite difference grid, into a set of subareas. The strain energy density for each subarea is then expressed in terms of displacement components and their derivatives. Next the derivatives are replaced by their finite difference equivalents, and the strain energy, together with the potential energy due to the applied loads, is summed over the shell surface. The total potential energy of the shell is then minimized according to familiar energy principles, and the resulting system of nonlinear algebraic equations is solved by a Newton-Raphson technique. The nonlinear shell theory of Ref. 30 is used, and the boundary conditions are rigorously satisfied. With the aid of user-written subroutines, very general initial imperfections can be introduced. In the present work the initial imperfections are taken to be similar to Eq. (21). Increments of load, increments of axial displacements, or increments of the "arc length" (see Ref. 31) can be used as the control parameter.

IV. Numerical Results

In the previous section the solution of the stochastic stability problem of Eq. (6) has been reduced to a series of $N + 1$ deterministic buckling load analyses. Several of the currently available structural analysis computer codes[27,32,33] have the capability of calculating the effect on buckling of given initial imperfections. However, as has been pointed out by Arbocz and Babcock[34] the success of such deterministic buckling load analysis depends very heavily on the appropriate choice of the model used, which in turn requires considerable knowledge by the user as to the physical behavior of the imperfect shell structure. This knowledge can best be acquired by first using the series of imperfection sensitivity analysis of increasing complexity that have been published in the literature.[1,2,35,36]

A. Characterization of Test Shells

For the statistical calculations the data associated with the integrally stringer stiffened aluminium alloy shells tested at CALTECH in 1969, the so-called AS-shells are used.[28] The shell properties are given in Table 1. For the numerical computations the properties of shell AS-2 are used.

Before the shells were buckled their initial imperfection was measured. Figure 2 displays the best-fit initial imperfection of shell AS-2.[28] The imperfection has been normalized by the shell thickness and is rolled out to show the circumferential and axial distribution. The largest deviation from the perfect shape is 0.93174 · h mm. It has been shown in Ref. 37 that for stringer stiffened shells satisfactory correlation between theoretical predictions and experimental results requires the inclusion of both the initial imperfections and the appropriate elastic boundary conditions in the analysis. To illustrate this effect reliability functions will be derived for SS-3 ($N_x = v = W = M_x = 0$), C-3 ($N_x = v = W = W_{,x} = 0$), and C-4 ($u = v = W = W_{,x} = 0$) boundary conditions. The collapse load calculations are done according to the approach recommended in Ref. 34, where it was pointed out that when one is studying the behavior of an imperfect shell it is necessary to determine first those buckling modes of the perfect shell that correspond to a few of the lowest buckling loads.

The buckling behavior of the stringer stiffened shell AS-2 has been studied extensively in the past (see Refs. 10, 34, 37). The results of Ref. 37 seem to indicate that the experimental boundary conditions of the test setup used to buckle the AS-shells at CALTECH[13] imposed elastic boundary conditions. This is contrary to the earlier belief that it approached closely the fully clamped C-4 boundary condition.

An eigenvalue map of modes calculated using nonlinear prebuckling with simply supported SS-3 boundary condition is shown in Table 2. A similar map for fully slamped C-4 boundary condition is displayed in Table 3. Notice that these tables identify by circumferential wave number and order of eigenvalue those modes that have buckling loads close to the lowest buckling load. Notice that the critical mode shapes may be symmetric or antisymmetric with respect to $x = L/2$. Thus in certain areas it may not be admissible to model only half the shell length.

Table 1 Geometric and material properties and experimental buckling loads of the AS-shells

	h, mm	A_1, mm^2	e_1, mm	$I_{11} \times 10^2$, mm^4	$I_{t1} \times 10^2$, mm^4	d_1, mm	P_{exp}, N
AS-2	0.1966	0.7987	0.3368	1.5038	4.9448	8.0239	14286.3
AS-3	0.2807	0.7432	0.3614	1.2033	4.0146	8.0289	22357.1
AS-4	0.2593	0.4890	0.2758	0.3474	1.2383	8.0112	17074.9

Note: For all shells, $E = 6.895 \times 10^4$ N/mm^2; $\nu = 0.3$; $R = 101.60$ mm; $L = 139.70$ mm; $NR \times NC = 21 \times 49$; 80 stringers.

Table 2 Buckling loads of the perfect AS-2 shell using nonlinear prebuckling (SS-3 boundary conditions: $N_x = v = W = M_x = 0$)

k	$l = 8$	9	10	11	12	13	14	15
1	1.2314	1.0416	1.000	1.0702	1.1791[a]	1.1390[a]	1.1475[a]	1.1944[a]
2	1.7877[a]	1.6158[a]	1.4292[a]	1.2756[a]	1.2190	1.3252	1.2995	1.2783
3	2.1203[a]	1.8867	1.7392	1.6002	1.4947	1.5140	1.5888[a]	1.5511[a]
4	2.3068	2.0466[a]	1.9570[a]	1.8530[a]	1.7459[a]	1.6546[a]	1.6553	1.7333

Note: All eigenvalues are normalized by −223.960 N/cm.
[a]Mode shape is antisymmetric at $x = L/2$.

Table 3 Buckling loads of the perfect AS-2 shell using nonlinear prebuckling (C-4 boundary conditions: $u = v = W = W_{,x} = 0$)

k	$l = 11$	12	13	14	15	16	17	18
1	1.1316	1.0881	1.0265[a]	1.0000[a]	1.0041[a]	1.0331[a]	1.0659	1.0949
2	1.1973[a]	1.0899[a]	1.0723	1.0583	1.0486	1.0504	1.0811[a]	1.1418[a]
3	1.3862	1.3182	1.3023	1.2576[a]	1.2286[a]	1.2159[a]	1.2188[a]	1.2381[a]
4	1.4518[a]	1.3685[a]	1.3038[a]	1.3413	1.3565	1.3515	1.3555	1.3688

Note: All eigenvalues are normalized by −316.890 N/cm.
[a]Mode shape is antisymmetric at $x = L/2$.

B. Analysis of Imperfect Shell

The buckling analysis of an imperfect shell can be carried out in a variety of ways with varying degrees of complexity. The purpose of this section is to determine the success of these types of analyses in predicting the buckling load of the test shell described in Sec. A. An additional purpose is to discover what each analysis has to contribute to the next level of analysis complexity.

The simplest type of imperfection sensitivity analysis is that introduced in Ref. 1 and further developed in Refs. 2, 10, and 38. In this analysis the sensitivity of the buckling load to a general single-mode asymmetric imperfection is studied. The results are expressed as

$$(1 - \rho_s)^{3/2} = (3/2)\sqrt{-3\alpha^2 b}[1 - (\beta/\alpha)(1 - \rho_s)]|\bar{\xi}| \quad (26)$$

where $\rho_s = N_s/N_c$, N_s is the limit load of the imperfect structure, $\bar{\xi}$ is the normalized amplitude of the initial imperfection, and N_c is the critical buckling load of the perfect shell. The second postbuckling coefficient b and the first and second imperfection form factors α and β are calculated with ANILISA.[38]

Assuming as a "worst type" of imperfection that W is in the form of (*affine* to) the lowest buckling mode, then

$$\overline{W} = \bar{\xi} h w(x) \cos \frac{ly}{R} \quad (27)$$

However, considering the measured initial imperfections of the shells shown in Figs. 2 and 3 one could also say that it appears from the Fourier representation of the measured data that sizeable imperfections can best be represented by the following trigonometric (*trig*) form:

$$\overline{W} = \bar{\xi} h \sin \frac{k\pi x}{L} \cos \frac{ly}{R} \quad (28)$$

where k and l are integers.

For the shell AS-2 ANILISA[38] yields the following results:

1) Using rigorous prebuckling analysis and $N_x = v = W = M_x = 0$ (SS-3) boundary conditions, for the *affine* imperfection of Eq. (27), $\alpha^2 b = -0.0254$, $\beta = 0.9395$; for the *trig* imperfection of Eq. (28), $\alpha^2 b = -0.0224$, $\beta = 0.9102$; with $k = 1$, $l = 10$.

Assuming that the amplitude of the imperfection is equal to the largest deviation from the perfect shape found in Fig. 2, then $\bar{\xi} = 0.932$ and Eq. (26) yields the following imperfect shell buckling loads: for the *affine* imperfection, $\rho_s = 0.616$; for the *trig* imperfection, $\rho_s = 0.618$. Notice that in this case $\rho_s = N_s/N_c$ is normalized by $N_c = -223.960$ N/cm, the critical buckling load of the perfect AS-shell using the SS-3 boundary conditions.

2) Using rigorous prebuckling analysis and $u = v = W = W_{,x} = 0$ (C-4) boundary conditions, for the *affine* imperfection of Eq. (27), $\alpha^2 b = -0.1552$, $\beta = 0.9711$; for the *trig* imperfection of Eq. (28), $\alpha^2 b = -0.0984$, $\beta = 0.7805$; with $k = 2$, $l = 14$.

Using once again $\bar{\xi} = 0.932$, the largest deviation from the perfect shape found in Fig. 2, then Eq. (26) yields the following imperfect shell buckling loads: for the *affine* imperfection, $\rho_s = 0.440$; for the *trig* imperfection, $\rho_s = 0.488$. It is important to remember that in this case $\rho_s = N_s/N_c$ is normalized by $N_c = -316.890$ N/cm, the critical buckling load of the perfect AS-2 shell using the C-4 boundary conditions.

Comparing the predicted buckling loads of $N_{SS\text{-}3} = -137.959$ N/cm and $N_{C\text{-}4} = -154.642$ N/cm based on the simple, single-mode, asymmetric imperfection model with the experimental buckling load of $N_{exp} = -223.793$ N/cm, one must conclude that the above predictions based on SS-3 or C-4 boundary conditions are overly conservative, especially for weight-sensitive applications. This implies that for better prediction a more detailed imperfection model must be used.

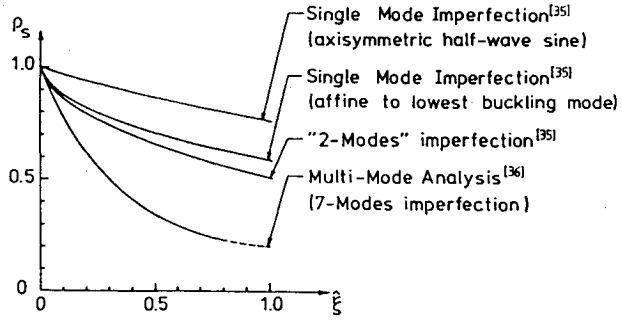

Fig. 11 Imperfection sensitivity for different imperfection models.

The imperfect shell AS-2 has been analyzed in the past using other models of various degrees of complexity. The most interesting results are displayed in Fig. 11. The interested reader should consult Refs. 10, 34, and 37 for further details and results.

C. Use of STAGS[27] to Derive Reliability Functions

The highest level of complexity in analysis is to use a two-dimensional nonlinear shell analysis code such as STAGS. With the use of this type of numerical tool one can, in principle, determine the buckling load of a complete shell structure including the effect of arbitrary prescribed initial imperfections represented by a double Fourier series. The computations reported in this paper were carried out with a STAGS-A code[27] modified so that besides increments of load and of axial displacement, increments of a "path parameter"[31] can be used as a loading parameter.

The number of imperfection modes included in the analysis is limited by practical considerations, like the time required for obtaining the solutions of all the buckling problems needed for the calculation of the derivatives $\partial\Psi/\partial\xi_j$. Thus, since the shell buckling load is determined by solving the governing equations for a particular set of initial imperfections, an attempt to select an optimal combination of these modes must be made. There is a need to identify those imperfection modes that dominate the prebuckling and the collapse behavior of the shell.

Examples of attempts to identify "critical imperfection modes," defined as that combination of axisymmetric and asymmetric imperfection modes that would yield the lowest buckling load, have been reported in the literature.[34-36] These studies have shown that in order to yield a decrease from the buckling load of the perfect structure, the initial imperfection harmonics used must include at least one mode with a significant initial amplitude and an associated eigenvalue that is close to the critical buckling load of the perfect structure. Relying on the results of earlier investigations of the buckling behavior of the imperfect AS-2 shell,[39] it was decided to use the following initial imperfection model for the collapse load calculations:

$$\begin{aligned}\overline{W} = {} & hA_{2,0}\cos\frac{2\pi x}{L} \\ & - h\sin\frac{\pi x}{L}(\bar{\xi}_{1,2}\cos 2\theta + \bar{\xi}_{1,9}\cos 9\theta + \bar{\xi}_{1,10}\cos 10\theta \\ & + \bar{\xi}_{1,11}\cos 11\theta + \bar{\xi}_{1,19}\cos 19\theta + \bar{\xi}_{1,21}\cos 21\theta)\end{aligned} \quad (29)$$

where $\bar{\xi}_{k,l} = \sqrt{C_{kl}^2 + D_{kl}^2}$ and $\theta = y/R$.

Notice that the shape of this imperfection model is symmetric in the axial direction about the center of the shell, hence only half of the shell length needs to be modeled.

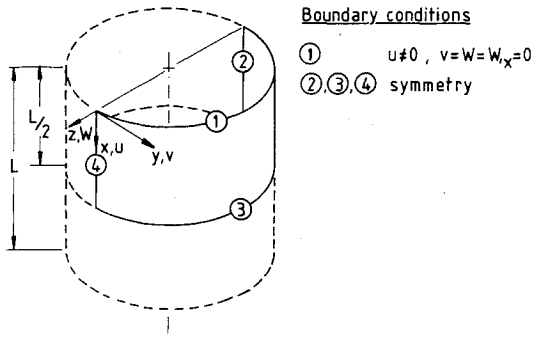

Fig. 12 Discrete shell model and the boundary conditions used.

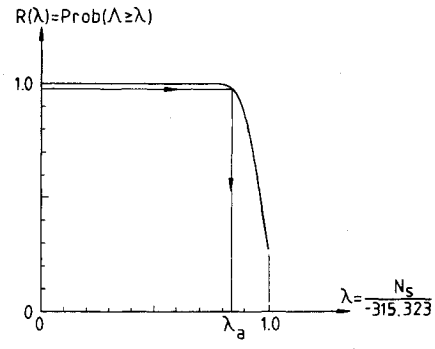

Fig. 13 Reliability curve calculated via the first-order, second-moment method (C-4 boundary condition: $u = v = W = W_x = 0$).

Table 4 Values of the equivalent Fourier coefficients and the reduced sample mean vector

	X_j	AS-2	AS-3	AS-4	$E(\ )$
$A_{2,0}$	1	0.00455	0.01378	−0.01126	0.00236
$\bar{\xi}_{1,2}$	2	0.33691	0.08298	0.54217	0.32069
$\bar{\xi}_{1,9}$	3	0.08843	0.02445	0.00297	0.03862
$\bar{\xi}_{1,10}$	4	0.05524	0.03148	0.00414	0.03028
$\bar{\xi}_{1,11}$	5	0.05494	0.01912	0.00502	0.02636
$\bar{\xi}_{1,19}$	6	0.01106	0.00689	0.00424	0.00740
$\bar{\xi}_{1,21}$	7	0.00879	0.00475	0.00095	0.00483

Table 5 Derivatives of ψ with respect to the equivalent Fourier coefficients (seven-mode imperfection model)

		$\partial\psi/\partial X_j$		
	X_j	SS-3	C-3	C-4
$A_{2,0}$	1	−0.6354	−0.6460	−0.5986
$\bar{\xi}_{1,2}$	2	0.1498	0.1522	0.1582
$\bar{\xi}_{1,9}$	3	0.6924	0.6863	0.3678
$\bar{\xi}_{1,10}$	4	0.9138	0.9344	0.6672
$\bar{\xi}_{1,11}$	5	0.6233	0.7390	1.0844
$\bar{\xi}_{1,19}$	6	0.2449	0.2795	0.2922
$\bar{\xi}_{1,21}$	7	0.1811	0.2591	0.4202

However, the imperfection model includes modes with both even and odd numbers of circumferential waves. This implies that in order to be able to use the symmetry conditions at $\theta = 0$ and $\theta = \Delta\theta$, half the shell perimeter must be modeled ($\Delta\theta = 180$ deg). Based on the results of convergence studies published earlier,[39] this leads to the use of the discrete model shown in Fig. 12 consisting of 21 × 131 mesh points. The above imperfection model requires eight collapse load calculations in order to be able to evaluate the derivatives $\partial\psi/\partial\xi_j$.

In order to apply the first-order, second-moment method, the mean buckling load has to be calculated first. Using the imperfection model of Eq. (29) with the mean values of the corresponding equivalent imperfection amplitudes listed in Table 4, the result of the calculation is $E(\Lambda_s) = 0.87538$, whereby the mean buckling load is normalized by −223.079 N/cm, the buckling load of the perfect AS-2 shell computed using nonlinear prebuckling and SS-3 boundary conditions.

In the following the derivatives $\partial\psi/\partial\xi_j$ are calculated. For the increment of the random variable in Eq. (14), 10% of the original mean value of the corresponding equivalent Fourier coefficient is used, so that $\Delta\xi_j = 0.10 \cdot E(X_j)$. The calculated derivatives are listed in Table 5. In this study the increments of the path parameter are chosen in such a way that the limit loads are found accurate to within 0.01%. Next, using the reduced sample variance-covariance matrix displayed in Table 6, one can evaluate the mathematical expectation and the variance of Z. The results of these calculations are $E(Z) = 0.87538\text{-}\lambda$ and $\mathrm{Var}(Z) = 0.00486$. Finally the reliability for SS-3 boundary conditions is calculated directly from Eq. (19) and is plotted in Fig. 10. Notice that for a reliability of 0.98 one obtains a knockdown factor of $\lambda_a = 0.73$, where in this case λ_a is normalized by −223.079 N/cm, the buckling load of the perfect AS-2 shell using nonlinear prebuckling and the SS-3 boundary conditions.

Switching now to the C-4 boundary conditions and using the same imperfection model as above, the calculated mean buckling load becomes $E(\Lambda_s) = 0.96298$, a value that is normalized by −315.323 N/cm, the buckling load of the perfect AS-2 shell computed using nonlinear prebuckling and the C-4 boundary conditions. Next, proceeding as described above, the derivatives $\partial\psi/\partial\xi_j$ are calculated. The values obtained are also listed in Table 5. The computation of the mathematical expectation and the variance of Z yield the values of $E(Z) = 0.96298\text{-}\lambda$ and $\mathrm{Var}(Z) = 0.00400$, respectively. Using Eq. (19) to calculate the reliability function $R(\lambda)$ for C-4 boundary conditions, the result is displayed in Fig. 13. Notice that in this case for a reliability of 0.98 one obtains a knockdown factor of $\lambda_a = 0.84$, where now λ_a is normalized by −315.323 N/cm, the buckling load of the perfect AS-2 shell using the C-4 boundary conditions.

Comparing the buckling loads predicted for a reliability of 0.98 of $N_{\text{SS-3}} = -162.848$ N/cm and $N_{\text{C-4}} = -264.871$ N/cm based on the seven-mode imperfection model of Eq. (29) with the experimental buckling load of $N_{\text{exp}} = -223.793$ N/cm, one notices that the calculated results seem to support the suggestion made in Ref. 37 that the experimental boundary conditions of the test setup used to buckle the AS-shells at CALTECH[13] imposed some sort of elastic boundary conditions.

Table 6 Reduced sample variance-covariance matrix (all terms are multiplied by 100)

	1	2	3	4	5	6	7
1	0.01604						
2	0.28485	5.29110			Symmetric		
3	−0.02165	−0.18590	0.19763				
4	−0.02122	−0.28341	0.10789	0.06537			
5	−0.01354	−0.12712	0.11436	0.06313	0.06625		
6	−0.00226	−0.02590	0.01511	0.00866	0.00879	0.00118	
7	−0.00303	−0.03884	0.01683	0.01001	0.00983	0.00134	0.00154

V. Conclusions

The results presented in this paper demonstrate conclusively that indeed it is possible to use the first-order, second-moment method to derive reliability-based improved knockdown factors for orthotropic shells under axial compression. In order to apply the method described in this study with confidence it is necessary that sufficient experimental data be available so that the statistical properties of the random variables involved can be estimated accurately.

A comparison of the improved knockdown factors λ_a obtained using SS-3 (see Fig. 10) and C-4 (see Fig. 13) boundary conditions illustrates very effectively the statement made in Ref. 39, that the key to the success of any stochastic stability analysis lies in the reliability and accuracy of the buckling load predictions made by the deterministic buckling analysis used. Thus, in cases where besides initial imperfection the collapse load of the structure is also greatly influenced by the type of boundary conditions used, one must model the experimental boundary conditions accurately. This may imply the need for using elastic boundary conditions in place of the idealized boundary conditions (SS-3 or C-4) used in this paper. For further details on this subject the interested reader should consult Refs. 5 and 40.

It is well known that the success of the deterministic buckling load analysis depends very heavily on the appropriate choice of the nonlinear model employed, which in turn requires considerable knowledge by the analyst of the expected physical behavior of imperfect shell structures. The authors wish to stress the fact that only a shell design specialist, who is aware of the latest theoretical developments and who is familiar with the theories upon which the nonlinear structural analysis codes that he or she uses are based, can achieve the accurate modeling of the collapse behavior of complex structures that guarantees a successful application of the method described in this study. The danger of incorrect predictions lies in the use of sophisticated computational tools by persons of inadequate theoretical background.

It must also be stressed that in this case the development of the proper numerical simulation procedure relies heavily on experimental data. Thus for a successful implementation of the proposed improved shell design procedure the companies involved in the production of shell structures must be prepared to do the initial investment in carrying out complete imperfection surveys on a small sample of shells that are representative of their production line. With the modern measuring and data acquisition systems complete surface maps of very large shells can be carried out, at a negligibly small fraction of their production cost.

That the proposed shell design procedure is also applicable to composite shells has been demonstrated in Ref. 41. In that case the random variables can represent not only initial imperfections but also other phenomena that have a random character, such as delamination buckling. Further, by using the appropriate numerical tools one can also include in the analysis, in addition to initial imperfections and (elastic) boundary conditions, other factors such as the effect of shear deformation or the effect of plastic yielding, if so desired.

Finally, it is believed that as the amount of data on characteristic initial imperfection distributions classified according to fabrication processes increases, one shall succeed with the modern tools of information science like data banks and computer networks to make the proposed improved shell design procedure available to more and more shell designers. Thus, finally, the engineering community will be able to point to the successful solution of one of the most perplexing problems in mechanics.

References

[1]Koiter, W. T., "On the Stability of Elastic Equilibrium," Ph.D. Thesis (in Dutch), TH-Delft, The Netherlands. H. J. Paris, Amsterdam, 1945; English translation NASA TTF-10, 1967, pp. 1–833.

[2]Budiansky, B., and Hutchinson, J. W., "Dynamic Buckling of Imperfection Sensitive Structures," *Proceedings of the 11th IUTAM Congress*, edited by H. Görtler, Springer-Verlag, Berlin, 1964, pp. 636–651.

[3]Hoff, N. J., "Buckling of Thin Shells," *Proceedings of an Aerospace Scientific Symposium of Distinguished Lecturers in Honor of Dr. Theodore von Kármán on his 80th Anniversary*, May 11, 1961, Inst. of Aeronautical Sciences, New York, 1962, pp. 1–86.

[4]Ohira, H., "Local Buckling Theory of Axially Compressed Cylinders," *Proceedings of the 11th Japan National Congress for Applied Mechanics*, Japan National Committee for Theoretical and Applied Mechanics, Science Council of Japan, Tokyo, 1961, pp. 37–40.

[5]Singer, J., and Rosen, A., "The Influence of Boundary Conditions on the Buckling of Stiffened Cylindrical Shells," *Proceedings of the IUTAM Symposium on Buckling of Structures*, edited by B. Budiansky, Springer-Verlag, Berlin, 1976, pp. 227–250.

[6]Anon., "Buckling of Thin-Walled Circular Cylinders," NASA SP-8007, 1968.

[7]Anon., "Rules for the Design, Construction and Inspection of Offshore Structures," DnV (Det norske Veritas), Oslo, Norway, 1977.

[8]Anon., "Beulsicherheitsnachweise für Schalen, DASt Richtlinie 013," Deutscher Ausschuss für Stahlbau, 1980.

[9]Weingarten, V. I., Morgan, E. J., and Seide, P., "Elastic Stability of Thin-Walled Cylindrical and Conical Shells Under Axial Compression," *AIAA Journal*, Vol. 3, No. 3, 1965, pp. 500–505.

[10]Arbocz, J., "Shell Stability Analysis: Theory and Practice," *Proceedings of the IUTAM Symposium on Collapse, the Buckling of Structures in Theory and Practice*, edited by J. M. T. Thompson and G. W. Hunt, Cambridge Univ. Press, New York, 1983, pp. 43–74.

[11]Singer, J., Abramovitch, H., and Yaffe, R., "Initial Imperfection Measurements of Stiffened Shells and Buckling Predictions," *Israel Journal of Technology*, Vol. 17, Nos. 5/6, 1979, pp. 324–338.

[12]Arbocz, J., "The Imperfection Data Bank, a Means to Obtain Realistic Buckling Loads," *Proceedings, Buckling of Shells—A State-of-the-Art Colloquium*, edited by E. Ramm, Springer-Verlag, Berlin, 1982, pp. 535–567.

[13]Singer, J., Arbocz, J., and Babcock, C. D. Jr., "Buckling of Imperfect Stiffened Cylindrical Shells Under Axial Compression," *AIAA Journal*, Vol. 9, No. 1, 1971, pp. 68–75.

[14]Imbert, J., "The Effect of Imperfections on the Buckling of Cylindrical Shells," Aeronautical Engineer Thesis, California Inst. of Technology, Pasadena, CA, 1971.

[15]Horton, W. H., "On the Elastic Stability of Shells, NASA CR-145088, 1977.

[16]Sebek, R. W. L., "Imperfection Surveys and Data Reduction of ARIANE Interstages I/II and II/III," ir. Thesis, Faculty of Aerospace Engineering, TU-Delft, The Netherlands, 1981.

[17]Green, D. R., and Nelson, H. M., "Compression Tests on Large-Scale, Stringer Stiffened Tubes," *Proceedings of the International Conference Buckling of Shells in Offshore Structures*, edited by P. J. Dowling and J. E. Harding, Granada, London, 1982, pp. 25–43.

[18]Grove, T., and Didriksen, T., "Buckling Experiments on 4 Large Axial Stiffened and 1 Ring Stiffened Cylindrical Shells," Det norske Veritas, Oslo, Rept. 76-432, 1976.

[19]Bolotin, V. V., "Statistical Methods in the Nonlinear Theory of Elastic Shells," Izvestija Akademii Nauk SSR, Otdelenie Tekhnicheskikh Nauk, No. 3, 1958; English translation NASA TTF-85, 1962, pp. 1–16.

[20]Fraser, W. B., and Budiansky, B., "The Buckling of a Column with Random Initial Deflections," *Journal of Applied Mechanics*, Vol. 36, No. 2, 1969, pp. 233–240.

[21]Amazigo, J. C., "Buckling Under Axial Compression of Long Cylindrical Shells with Random Axisymmetric Imperfections," *Quarterly Journal of Applied Mathematics*, Vol. 26, No. 4, 1969, pp. 537–566.

[22]Roorda, J., "Some Statistical Aspects of the Buckling of Imperfection-Sensitive Structures," *Journal of Mechanics and Physics of Solids*, Vol. 17, No. 1, 1969, pp. 111–123.

[23]Hansen, J., "General Random Imperfections in the Buckling of Axially Loaded Cylindrical Shells," *AIAA Journal*, Vol. 15, No. 9, 1977, pp. 1250–1256.

[24]Elishakoff, I., "Buckling of a Stochastically Imperfect Finite Colume on a Nonlinear Elastic Foundation—A Reliability Study," *Journal of Applied Mechanics*, Vol. 46, No. 2, 1979, pp. 411–416.

[25]Elishakoff, I., Manen, S. van, Vermeulen, P. G., and Arbocz, J., "First-Order Second-Moment Analysis of the Buckling of Shells with Random Imperfections," *AIAA Journal*, Vol. 25, No. 8, 1987, pp. 1113–1117.

[26]Karadeniz, H., Manen, S. van, and Vrouwenvelder, A., "Probabilistic Reliability Analysis for the Fatigue Limit State of Gravity

and Jacket Type Structures," *Proceedings of the Third International Conference on Behavior of Off-Shore Structures*, McGraw-Hill, London, 1982, pp. 147–165.

[27]Almroth, B. O., Brogan, F. A., Miller, E., Zelle, F., and Peterson, H. T., "Collapse Analysis for Shells of General Shape," *User's Manual for the STAGS-A Computer Code*, Air Force Flight Dynamics Lab., Wright-Patterson AFB, AFFDL-TR-71-8, 1973.

[28]Arbocz, J., and Abramovich, H., "The Initial Imperfection Data Bank at the Delft University of Technology—Part I," Rept. LR-290, Delft Univ. of Technology, Dept. of Aerospace Engineering, The Netherlands, 1979.

[29]Abramovich, H., Singer, J., and Yaffe, R., "Imperfection Characteristics of Stiffened Shells—Group 1," TAE Rept. 406, Dept. of Aeronautical Engineering, Technion, Israel Inst. of Technology, Haifa, Israel, 1981.

[30]Marlow, M. B., and Flügge, W., "Some New Developments in the Foundation of Shell Theory," Rept. LMSC 6-78-68-13, Lockheed Missiles & Space Co., Palo Alto, CA, 1968.

[31]Riks, E., "Some Computational Aspects of the Stability Analysis of Nonlinear Structures," *Computer Methods in Applied Mechanics and Engineering*, Vol. 47, 1984, pp. 219–259.

[32]Anon., "ABAQUS—Theory Manual," Version 4.6, Hibbitt, Karlsson & Sorensen, Inc., Providence, RI.

[33]Anon., "MSC/NASTRAN—User's Manual, Vol. I," The MacNeal-Schwendler Corp., Los Angeles, CA.

[34]Arbocz, J., and Babcock, C. D., "The Buckling Analysis of Imperfection Sensitive Structures," NASA CR-3310, Aug. 1980.

[35]Arbocz, J., "The Effect of Initial Imperfections on Shell Stability," *Proceedings Thin-Shell Structures, Theory Experiment and Design*, edited, by Y. C. Fung and E. E. Sechler, Prentice-Hall, Englewood Cliffs, NJ, 1974, pp. 205–245.

[36]Arbocz, J., and Babcock, C. D., "Prediction of Buckling Loads Based on Experimentally Measured Initial Imperfections," *Proceedings of the IUTAM Symposium Buckling of Structures*, edited by B. Budiansky, Springer-Verlag, Berlin, 1976, pp. 291–311.

[37]Arbocz, J., "Collapse Load Calculations for Axially Compressed Imperfect Stringer Stiffened Shells," *Proceedings of the AIAA/ASME/ASCE/AHS 25th Structures, Structural Dynamics and Materials Conference*, May 14–18, 1984, Palm Springs, CA, AIAA, New York, pp. 130–139.

[38]Arbocz, J., and Hol, J. M. A. M., "ANILISA—Computational Module for Koiter's Imperfection Sensitivity Theory," Rept. LR-582, Delft Univ. of Technology, Faculty of Aerospace Engineering, The Netherlands, 1989.

[39]Arbocz, J., and Babcock, C. D., "Utilization of STAGS to Determine Knockdown Factors from Measured Initial Imperfections," Rept. LR-275, TH-Delft, Dept. of Aerospace Engineering, The Netherlands, Nov. 1978.

[40]Singer, J., "Vibrations and Buckling of Imperfect Stiffened Shells—Recent Developments," *Proceedings of the IUTAM Symposium on Collapse, The Buckling of Structures in Theory and Practice*, edited by J. M. T. Thompson and E. W. Hunt, Cambridge Univ. Press, New York, 1983, pp. 443–479.

[41]Arbocz, J., and Hol, J. M. A. M., "The Role of Experiments in Improving the Computational Models for Composite Shells," *CED—Vol. 3, Analytical and Computational Models of Shells*, edited by A. K. Noor, T. Belytschko, and J. C. Simo, American Society of Mechanical Engineers, New York, 1989.